Available online at www.sciencedirect.com
ScienceDirect
Journal of Nuclear Materials 376 (2008) 282–288
journal of nuclear materials
www.elsevier.com/locate/jnucmat

High temperature oxidation of Fe–9Cr–1Mo steel in stagnant liquid lead–bismuth at several temperatures and for different lead contents in the liquid alloy

L. Martinelli [a,*], T. Dufrenoy [a], K. Jaakou [b], A. Rusanov [c], F. Balbaud-Célérier [a]

[a] *Service de la Corrosion et du Comportement des Matériaux dans leur Environnement, CEA-Saclay, DEN/DPC/SCCME/LECNA, Bât. 458 Point courrier n°50, 91191 Gif sur Yvette cedex, France*
[b] *Service de Recherches Métallurgiques Appliquées, CEA/Saclay, 91191 Gif sur Yvette cedex, France*
[c] *IPPE, Bondarenko Square 1, Obninsk, 249020 Kaluga Region, Russia*

Abstract

This research project deals with the feasibility studies concerning the construction of an hybrid reactor for the transmutation of long-lived radioactive wastes. In this context, the liquid lead–bismuth eutectic (LBE) is considered to be a good candidate for the spallation target material needed for the neutrons production necessary to the transmutation. In this hybrid reactor, the LBE, which is enclosed in a T91 (Fe–9%Cr) steel container, can induce corrosion concerns. If the oxygen content dissolved in Pb–Bi is higher than the needed content for magnetite formation, corrosion proceeds by oxidation of the steel. Previously, specific results were reported, obtained in stagnant liquid LBE at 470 °C. An analytical model taking into account the oxide layer structure has been carried out. It involves iron, oxygen and chromium bulk diffusion and diffusion via preferential paths such as liquid lead–bismuth nano-channels incorporated in the oxide layer structure and grain boundaries. In this paper, experimental results on corrosion kinetics, obtained at different temperatures with different percentages of lead in the lead–bismuth alloy, are presented. The model, adapted to the different experimental conditions, is compared to these kinetics and to experimental points coming from the literature at different temperatures in LBE, in pure lead and in pure bismuth.

PACS: 81.65.Mq

1. Introduction

Accelerator-driven Systems are a technical option for transmuting long-lived nuclear wastes. In such systems, protons generated by an accelerator impinge on a target to produce neutrons through a spallation process. These neutrons are then used for waste transmutation. Flowing liquid metals are primary candidates for the spallation target material, due to the high power density deposited by the proton beam. Among liquid alloys, the Pb–Bi eutectic (LBE), Pb–55 at.%Bi, appears to be a good candidate, due to its high atomic number, low melting point (125 °C), fast heat removal from the target, good neutron yield and low vapour pressure. However, liquid metals can be corrosive towards containment materials (austenitic steels and Fe–9Cr alloys). The T91 (Fe–9Cr) martensitic steel has been chosen to be the structure material for the hottest part of the reactor. T91 corrosion considerations, in the operating and accidental temperature range (350–600 °C), are thus essential for the structures proportioning. However, the operating conditions are not completely defined in the reactor, the chemical state of the liquid alloy is not known (dissolved oxygen content, temperature gradient...). The objective of this work is to predict the oxidation of the T91 considering that some of the physico-chemical properties of the Pb–Bi alloy can locally evolve in the reactor: the dissolved oxygen and iron concentrations, the temperature and the proportions of lead and bismuth in the liquid alloy.

* Corresponding author. Tel.: +33 1 69 08 16 13; fax: +33 1 69 08 15 86.
E-mail address: laure.martinelli@cea.fr (L. Martinelli).

0022-3115/$ - see front matter © 2008 Elsevier B.V. All rights reserved.
doi:10.1016/j.jnucmat.2008.02.006

Nomenclature

$a_{O_2}^{mag/Pb-Bi}$ oxygen activity at the magnetite/Pb–Bi interface
$a_{O_2}^{sp/mag}$ oxygen activity at the Fe–Cr spinel/magnetite interface
$a_{O_2}^{T91/sp}$ oxygen activity at the T91/ Fe–Cr spinel interface
a_X activity of the element X
C_{Fe}^{mag} iron concentration in the magnetite layer (mol/cm^3)
C_{Fe}^{sp} iron concentration in the Fe–Cr spinel layer (mol/cm^3)
C_{Fe}^{T91} iron concentration in the T91 (mol/cm^3)
$D_{Fe}^{Magnetite}$ iron diffusion coefficient determined by Backhaus-Ricoult and Dieckmann in magnetite lattice (cm^2/s) [15]
$D_{Fe}^{mag,\ Topfer}$ iron diffusion coefficient determined by Töpfer, Aggarwal and Dieckmann in the magnetite lattice at 1200 °C (cm^2/s) [14]
$D_{Fe}^{sp,Topfer}$ iron diffusion coefficient determined by Töpfer, Aggarwal and Dieckmann in the $Fe_{2.4}Cr_{0.6}O_4$ spinel lattice at 1200 °C (cm^2/s) [14]
D_I interstitials diffusion coefficient (cm^2/s)
D_V vacancies diffusion coefficient (cm^2/s)
$\Delta G_f^0(X)$ formation free enthalpy of the compound X (J/mol)
h oxide scale thickness (μm)
h_{mag} magnetite thickness (μm)
K_I reaction constant leading to the formation of an interstitial
K_p parabolic constant (μm^2/h, or cm^2/s)
K_p^0 pre-exponential constant of the parabolic constant (cm^2/s)
K_V reaction constant leading to the formation of a vacancy
P_{O_2} oxygen partial pressure (bar, atm)
$P_{O_2}^0$ reference oxygen partial pressure (bar, atm)
Q activation energy of the parabolic constant (J)
R gaseous constant (J/mol/K)
t oxidation time (h)
T temperature (K)
x_{Pb} lead molar fraction in Pb–Bi alloy

In a previous work, a predictive model of T91 oxidation in oxygen saturated liquid LBE has been performed at 470 °C [1–4]. This model can be adapted for other experimental conditions (dissolved oxygen content or lead activity in oxygen saturated conditions) and extrapolated at other temperatures. In this paper, the T91 oxidation is studied for different Pb–Bi environments: for LBE at different temperatures and for liquid Pb–Bi with different contents of lead. The model [3,4] is extrapolated for different temperatures and different lead contents in the liquid Pb–Bi alloy and then compared to the experimental results of this study and to the literature data. The impact of these two physico-chemical parameters (temperature and lead content in Pb–Bi) on the T91 oxidation rate is then discussed.

2. Experimental

2.1. Sample and oxidation treatments

Tests are performed using martensitic steel T91 (chemical composition (wt%): 9% Cr, 1% Mo, 0.18–0.25% V, 0.1% C and 0.06–0.10% Nb) mechanically polished until 1200 grit SiC paper before the oxidation experiments. Samples dimensions are 30 mm × 10 mm × 1 mm. Oxidation experiments are performed after the same surface preparation, in oxygen saturated conditions, at different temperatures and different contents of lead in the lead–bismuth alloy.

The tests temperatures are 460 °C (3 oxidation times: from 230 h to 780 h), 550 °C (1 oxidation time: 260 h) 600 °C (3 oxidation times: from 350 h to 1000 h) and 630 °C (5 oxidation times: from 110 h to 710 h). Some experimental problems occurred with the temperature acquisition system of the facility in which the 460 °C and the 630 °C tests were performed. The temperature values are thus not precisely known. These temperatures are considered to be 460 °C and 630 °C as a post test was performed with an external thermocouple, using the same settings as during the oxidation test. Tests are carried out in a glove box, in crucibles made of preoxidised 316 L for experiments at 460 °C and 630 °C and in aluminized 316 L crucibles for the others. The glove box gaseous atmosphere is dry air for experiments at 460 °C and 630 °C and argon for the others. To verify that the oxygen content is at the saturation level during the whole test, the oxygen content dissolved in Pb–Bi is continuously measured by a specific oxygen sensor made of yttria stabilised zirconia (supplied by Umicore) [5]. Due to oxygen saturation, a lead oxide layer always covered the liquid metal surface.

The durations of the oxidation tests are always lower than 1000 h: T91 samples are immersed in Pb–Bi alloy during a determined time, removed from Pb–Bi and quenched in the glove box atmosphere. After quenching, the samples are observed by scanning electron microscopy (SEM) and analysed by Castaing microprobe and SEM/EDX.

2.2. Oxidation kinetics

Figs. 1 and 2 show the results of the oxidation tests performed in oxygen saturated Pb–Bi at 460 °C in 36Pb–64 Bi, 600 °C in Pb–Bi eutectic (LBE) and 630 °C in 26Pb–74Bi.

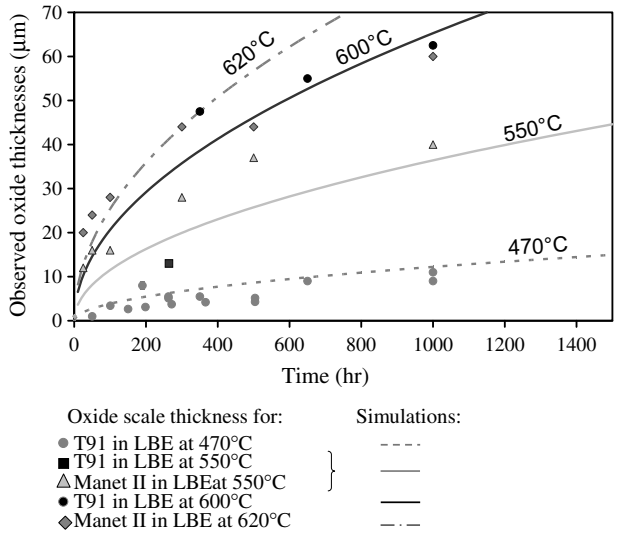

Fig. 1. growth rate of oxide scale obtained by oxidation of T91 in oxygen saturated Pb–Bi eutectic at 470 °C [3,4], 550 °C (1 point) and 600 °C and by oxidation of Manet II(Fe–10.3Cr) in oxygen saturated Pb–Bi eutectic at 550 °C and 620 °C [6].

The oxide scale thicknesses measured, on sample cross section by SEM, are quite thick. These thicknesses are equal to 9 μm after 780 h immersion in 36Pb–64Bi alloy at 460 °C, to 62 μm after 1000 h immersion in LBE at 600 °C and to 90 μm after 710 h immersion in 26Pb–74Bi alloy at 630 °C.

Fig. 1 shows that the oxidation kinetics increases when the temperature increases. Therefore the kinetics at 600 °C is faster than the oxidation kinetics obtained at 470 °C [2] and 550 °C [6] and slower than the oxidation kinetics measured at 620 °C [6].

2.3. Oxide scale analyses

According to the literature [2,5,7,8,10,12,11], the oxidation of Fe–(9 or 10.3)Cr steels in liquid Pb–Bi leads to the formation of a duplex oxide scale in which some lead penetrations have been observed. This duplex oxide scale is constituted of an internal Fe–Cr spinel layer in contact with T91 and an external magnetite layer in contact with Pb–Bi. The nature of these two layers is the same whatever the temperatures are between 470 °C and 600 °C and the Pb–Bi alloy composition. The thickness ratio between the two oxide scales is approximately equal to one (according to [2] the magnetite layer is 1.2 times thicker than the Fe–Cr spinel layer). The magnetite layer contains cavities. The Fe–Cr spinel stoichiometry has been measured at 470 °C [2]. The Fe–Cr spinel stoichiometry is $Fe_{2.3}Cr_{0.7}O_4$ in the whole Fe–Cr spinel layer and whatever the oxidation duration. Actually the chromium volume concentration is the same in the steel and in the Fe–Cr spinel, and this characteristic fixes the Fe–Cr spinel stoichiometry [2].

As it was observed previously [2,5,7,8,10,12,11], the specimens oxidised at 460, 550, 600 and 630 °C present a double scale microstructure, which is revealed by SEM (Fig. 4). Some cavities are found in the upper layers (Fig. 4).

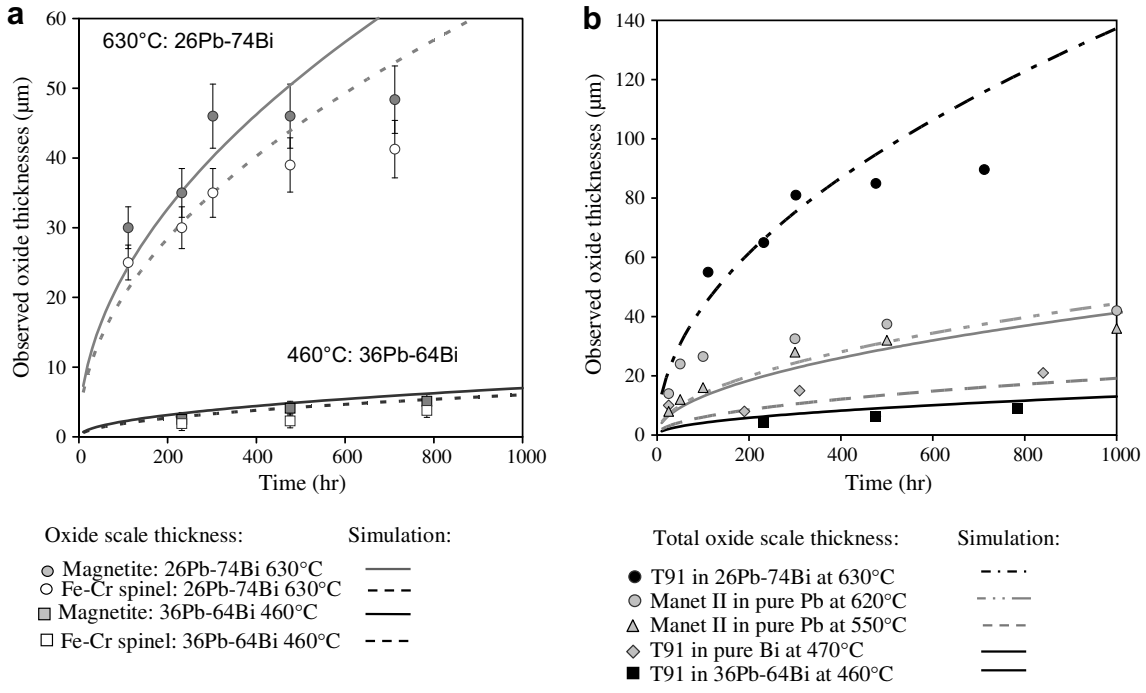

Fig. 2. (a) growth rate of oxide scale obtained by oxidation of T91 in oxygen saturated 36Pb–64Bi alloys at 460 °C and in oxygen saturated 26Pb–74Bi alloys at 630 °C with their corresponding simulations. (b) growth rate of oxide scale obtained by oxidation of T91 in oxygen saturated 36Pb-64Bi alloys at 460 °C, in 26Pb–74Bi alloys at 630 °C, in pure Bi at 470 °C [3] and of Manet II in pure Pb at 550 °C and 620 °C [6]. Corresponding simulations.

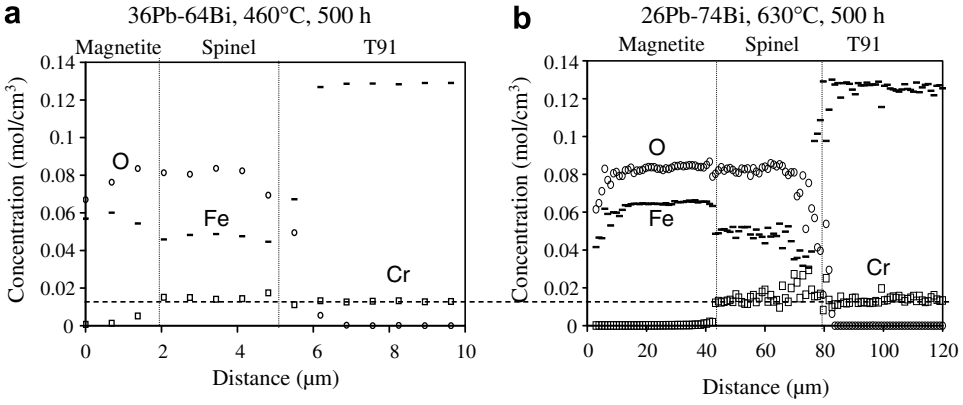

Fig. 3. microprobe profiles of T91 cross sections of T91 samples oxidized 500 h in 36Pb–64Bi at 460 °C, (a) and 500 h in 26Pb–74Bi at 630 °C (b).

The upper oxide scale is approximately 1.1 times thicker than the inner oxide scale whatever the oxidation time is and the temperature of the test. The chemical composition of the scales is obtained by Castaing microprobe analyses (Fig. 3). Inside the oxide scale the atomic percent ratio between the cations (iron plus chromium) and the anion (oxygen) is equal to 3/4: the spinel structure $(FeCr)_3O_4$ can thus be assumed. The oxide layer in contact with the liquid Pb–Bi alloy is magnetite (Fe_3O_4) as it contains only iron and oxygen. The oxide layer in contact with T91 is an Fe–Cr spinel the stoichiometry of which is calculated and equal to $Fe_{2.3}Cr_{0.7}O_4$ (Fig. 3). Indeed, Fig. 3 shows that the chromium volume concentrations in the Fe–Cr spinel scale and in the T91 are equal. However, chromium enrichment is observed at the Fe–Cr spinel/T91 interface on Fig. 3(b).

To conclude, all the characteristics of the oxide scales observed in literature [2,5,7,8,10,12,11] are also observed in the present tests.

3. Discussion

The oxide scale characteristics are the same in this study and in [2]. Consequently the same oxidation mechanism can be assumed and the model corresponding to this mechanism [3] can be applied. In this model the oxide growth rate is considered to be controlled by the iron diffusion in the oxide scale. The iron coefficient diffusion is extrapolated from high temperatures (in the 1000 °C range) [15] to the studied temperature range (400–650 °C) [3]. The model, allowing to calculate the magnetite and the Fe–Cr spinel layers thicknesses during time, just depends on temperature and oxygen content in the liquid alloy. It can easily be applied to experiments at different temperatures (see Section 3.2.1) but it does not depend on the Pb–Bi alloy composition (see Section 3.2.2). However in the case of the oxidation tests in different oxygen saturated Pb–Bi alloys, the oxygen content dissolved in Pb–Bi alloy changes when the Pb–Bi alloy composition changes as the oxygen solubility limit depends on the alloy composition. Consequently in the case of the oxidation tests in different oxygen saturated Pb–Bi alloys, the model varying parameter is the oxygen content in the liquid Pb–Bi alloy. The model calculation bases are presented in Section 3.1 and then adapted to the experimental conditions of this study and to the ones of the literature [2,3,6]: T91 this study [2,3] and Manet II [6] oxidation in oxygen saturated LBE at several temperatures and this study [3] and Manet II [6] oxidation in oxygen saturated Pb–Bi alloy containing different contents of lead (see Section 3.2). The effect of the temperature increase on the oxidation rate is firstly discussed (see Section 3.2.1). The model is then applied to oxidation tests in different Pb–Bi alloys (see Section 3.2.2) to study the impact of the alloy composition on the oxidation rate.

3.1. Calculation

The model proposed in [3] forecasts the magnetite scale thickness according to the expressions (1) and (2). The magnetite thickness is written:

- as a function of time and as a function of the oxygen activities at the magnetite/liquid Pb–Bi and the Fe–Cr spinel/magnetite interfaces in expression (1),
- as a function of time and as a function of the oxygen activities at the Fe–Cr spinel/magnetite and the Fe–Cr spinel/T91 interfaces in expression (2)

$$h_{\mathrm{mag}}^2 = \left[\frac{Dv}{12}\ln\left(\frac{1+2K_v a_{O_2}^{\mathrm{mag/Pb\text{–}Bi}^{2/3}}}{1+2K_v a_{O_2}^{\mathrm{sp/mag}^{2/3}}}\right) - \frac{8}{3}D_I K_I\left(a_{O_2}^{\mathrm{mag/Pb\text{–}Bi}^{-2/3}} - a_{O_2}^{\mathrm{sp/mag}^{-2/3}}\right)\right]t \quad (1)$$

$$h_{\mathrm{mag}}^2 = \frac{2}{2.4}A\left[\frac{D_{\mathrm{Fe}}^{\mathrm{sp,\ Topfer}}}{D_{\mathrm{Fe}}^{\mathrm{mag,\ Topfer}}}(V)\frac{Dv}{8}\ln\left(\frac{1+2K_v a_{O_2}^{\mathrm{sp/mag}^{2/3}}}{1+2K_v a_{O_2}^{\mathrm{T91/sp}^{2/3}}}\right) - 4\frac{D_{\mathrm{Fe}}^{\mathrm{sp,\ Topfer}}}{D_{\mathrm{Fe}}^{\mathrm{mag,\ Topfer}}}(I)D_I K_I\left(a_{O_2}^{\mathrm{sp/mag}^{-2/3}} - a_{O_2}^{\mathrm{T91/sp}^{-2/3}}\right)\right]t. \quad (2)$$

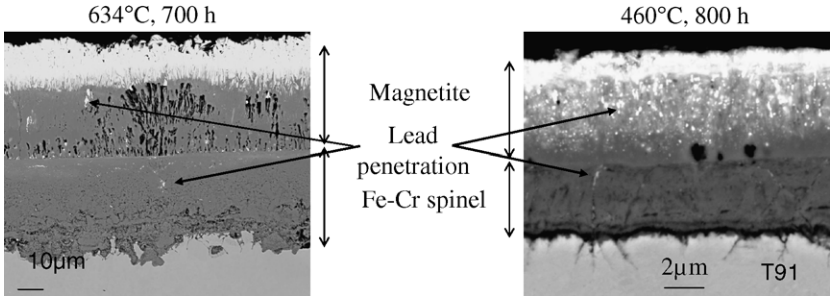

Fig. 4. SEM pictures of T91 cross sections of T91 samples oxidized 800 h in 36Pb–64Bi at 460 °C and 700 h in 26Pb–74Bi at 630 °C.

With $A = \frac{C_{Fe}^{sp}(C_{Fe}^{T91} - C_{Fe}^{sp})}{C_{Fe}^{mag^2}}$.

The equality between expressions (1) and (2) allows the determination of the value of the oxygen activity at the magnetite/Fe–Cr spinel interface, as all the other parameters are known.

Afterwards, the calculation of magnetite thickness can equally be performed with expression (1) or (2) using the following values for oxygen activities at the Pb–Bi/magnetite and the Fe–Cr spinel/T91 interfaces

- $a_{O_2}^{mag/Pb-Bi}$: oxygen activity corresponding to the oxygen partial pressure in equilibrium with the oxygen saturated liquid Pb–Bi. This activity is: $a_{O_2} = a_{Pb}^{-2} \exp\left(\frac{2\Delta G_f^0(PbO)}{RT}\right)$. Considering that $a_{PbO}^0 = 1$ for PbO in its solid phase and $a_{Pb} = x_{Pb} \exp\left(-\left(\frac{447}{T} + 0.2\right)(1 - x_{Pb})^2\right)$ [17] (3).
- $a_{O_2}^{T91/sp}$: because of the Fe–Cr spinel growth process [2–4], this oxygen activity is the one in equilibrium with T91 and Fe_3O_4. It is calculated with literature data [16], assuming ideal solution (iron activity equal to 0.9 inside T91).

The magnetite layer thickness can thus be determined with the numerical data given in Tables 1 and 2 using Eqs. (1) and (2).

According to [2] the Fe–Cr spinel layer thickness is calculated from the magnetite layer thickness considering the following expression:

$$h_{sp} = \frac{C_{Fe}^{mag}}{C_{Fe}^{T91} - C_{Fe}^{sp}} h_{mag}. \quad (3)$$

3.2. Results and discussion

3.2.1. Temperature effect

Fig. 1 shows the experimental points and the simulations performed for each temperature, considering oxygen saturated LBE. Due to the increase of the iron diffusion coefficient as the temperature increases (see Tables 1), the simulated growth rate also increases. The same temperature dependence is observed on the oxidation tests. Moreover, experiments and simulations are quantitatively in very good agreement. This leads to two conclusions:

- The simulation, established from the T91 oxidation mechanism at 470 °C in oxygen saturated LBE [2,3], also forecasts the oxidation kinetics of T91 and Manet II (Fe–10.3Cr) at 550 °C, Manet II at 620 °C and T91 at 600 °C.
- The same oxidation mechanism can thus be considered for the two martensitic Fe–9Cr and Fe–10.3Cr steels in the temperature range 470–620 °C in oxygen saturated conditions.

Consequently, this leads to conclude that the temperature dependence of the iron diffusion coefficient in magnetite and Fe–Cr spinel is reliably extrapolated from high temperature [14,15] to the temperature range of this study.

Moreover, the good agreement between the simulated parabolic constant and each experimental parabolic constant leads to conclude that the temperature effect on the oxide growth rate is just due to the thermal activation of iron diffusion in the oxide scale.

3.2.2. Effect of lead content in the liquid Pb–Bi alloy

According to the model, the composition of the liquid alloy does not contribute to the oxidation mechanism. However, because the oxygen solubility limit in the Pb–Bi alloy depends on the alloy lead content, the liquid alloy composition fixes the oxygen activity at the magnetite/Pb–Bi interface in the case of oxygen saturated conditions. Indeed, the oxygen solubility limit varies in the liquid alloy according to expression (1) and the oxygen solubility limit in pure bismuth is higher than the one in pure lead.

Table 1
Numerical data used for the simulation of the magnetite layer growth

	460 °C in 36Pb–64Bi	550 °C in Pb	550 °C in LBE	600 °C in LBE	620 °C in Pb	620 °C in LBE	630 °C in 26Pb–74Bi
$a_{O_2}^{mag/Pb-Bi}$	2.4×10^{-20}	4.3×10^{-18}	3.2×10^{-17}	1.2×10^{-15}	6.6×10^{-16}	4.8×10^{-15}	3.8×10^{-14}
$a_{O_2}^{T91/sp}$	9.7×10^{-32}	1.8×10^{-27}	1.8×10^{-27}	1.7×10^{-25}	9.4×10^{-25}	9.5×10^{-25}	2.1×10^{-24}
$a_{O_2}^{sp/mag}$	1.0×10^{-20}	1.6×10^{-18}	1.3×10^{-17}	4.9×10^{-16}	2.1×10^{-16}	1.9×10^{-15}	1.5×10^{-14}
a_{Pb}	0.26	1	0.36	0.37	1	0.37	0.18

Table 2
List of values of the different parameters necessary for the iron diffusion coefficient calculation in magnetite [15]

Vacancies diffusion coefficient: $D_v = 0,177\eta \exp\left(\frac{-14600}{T}\right) + 1.16 \times 10^{-3}(1-\eta)\exp\left(\frac{-8670}{T}\right)$ and $\eta = \frac{1}{\left(1+3\times 10^3 \exp\left(\frac{11900}{T}\right)\right)}$
Interstitial diffusion coefficient: $D_i = \frac{1{,}22\times 10^4 \exp\left(\frac{-27700}{T}\right)}{\left(1+1.56\times 10^6 \exp\left(\frac{-20100}{T}\right)\right)}$
$K_v = 2.04 \times 10^{-7}\exp\left(\frac{27170}{T}\right)$ and $K_i = 1.93 \times 10^9 \exp\left(\frac{-43140}{T}\right) + 3.10 \times 10^9 \exp\left(\frac{-63270}{T}\right)$ are the reaction constants leading respectively o he formation of a vacancy and an interstitial site
With $a^0_{O_2} = \frac{P_{O_2}}{P^0_{O_2}}$ and $P^0_{O_2} = 1$bar

It means that higher is the lead content in the Pb–Bi alloy, the lower the simulated oxide growth rate is.

Fig. 2(a) shows the simulations performed for Fe–Cr spinel and magnetite scales in 26Pb–74Bi and in 36Pb–64Bi, together with experimental values of magnetite and Fe–Cr spinel thicknesses.

Fig. 2(b) presents:

- some experimental oxide thicknesses, coming from [3,6], obtained by oxidation of T91 and Manet II, respectively in oxygen saturated pure bismuth and oxygen saturated pure lead,
- the experimental oxide thicknesses obtained in this study in oxygen saturated 26Pb–74Bi at 630 °C and in oxygen saturated 36Pb–64Bi at 460 °C,
- the simulations parametrized according the experimental tests conditions and performed following the previous calculation (see Section 3.1); the numerical data used for the simulations are given in Tables 1 and 2,
- simulation in oxygen saturated pure bismuth at 470 °C coming from [3].

Fig. 2(a) shows that the simulations match with the experimental thicknesses of magnetite and Fe–Cr spinel however a shift is observed for the fourth experimental point in 26Pb–74Bi at 500 h. This simulation deviation from the experimental points could be due to the chromium enrichment observed at the Fe–Cr spinel/T91 interface (Fig. 3(b)). Indeed, the vacancy diffusion coefficient decreases when the chromium concentration increases in the Fe–Cr spinel. A diffusion barrier can then be carried out at the Fe–Cr spinel/T91 interface for the long time experiments at high temperature. In agreement with the simulation, for approximately the same temperature range (460–470 °C and 620–630 °C, Fig. 2(b)) the experimental growth rate is higher:

- for the oxygen saturated pure bismuth environment (470 °C) than for the oxygen saturated 36Pb–64Bi,
- and for the oxygen saturated 26Pb–74Bi (630 °C) than for the oxygen saturated pure lead (620 °C).

For pure bismuth, the simulation is in good agreement with the three first experimental points, the oxide thickness of the fourth is shift to the half of the simulation. It is difficult to conclude only from four points, more experimental points would be necessary to complete this kinetics and to conclude on the validity of the simulation in that case.

For pure lead, the experimental kinetics at 620 °C matches very well with the simulation. On the other hand, the experimental kinetics at 550 °C is not in agreement with the simulation. Moreover, Fazio et al. [9] performed oxidation tests on Mod F82H (Fe–7.8Cr) in oxygen saturated pure lead at 464 °C during 700 and 1200 h. The total oxide thickness is 8 μm after 700 h and 20 μm after 1200 h (not represented on Fig. 2). If we compare these results to these obtained in LBE, we can see that at 1200 h the oxide layer measured in pure lead (20 μm) is much higher than the simulated one in LBE (13 μm). According to the simulation hypotheses [3,4], the simulated growth rate in pure lead is slower than the one in LBE and thus the simulated thickness in pure lead is lower than the experimental one in pure lead after 1200 h. Consequently, the simulation always underestimates the corrosion rate in case of oxidation in pure lead, except for experiments at 620 °C. Therefore, more complete experimental kinetics should be performed to obtain coherent oxidation data in pure lead and to conclude on the validity of the model in case of pure lead.

To conclude on the lead content effect on the Fe–9Cr oxidation in Pb–Bi alloy, the experimental points are in good agreement with the simulation in case of lead alloy containing bismuth: for 36Pb–64Bi, for the 3 first points in 26Pb–74Bi, for the 3 first points in pure bismuth. As the last points always shift from the simulation (except for 36Pb–64Bi), a longer kinetics is needed to determine if this shift is just coincidence or if it corresponds to a kinetics change (and thus to a change in the oxidation mechanism). In the case of oxidation in pure lead, the simulation, in comparison with experimental tests, underestimates the oxidation rate with Manet II at 550 °C [6] and Mod F82H at 464 °C [9] (not shown in Fig. 2). On the other hand agreement is obtained between our simulation and experiments in pure lead at 620 °C [6]. Longer experimental kinetics are thus needed to conclude on the Pb–Bi composition impact on the oxidation rate. The relatively good agreement for 36Pb–64Bi, 26Pb–74Bi, pure bismuth and pure lead at 620 °C allows to propose that the composition of the liquid alloy impacts the corrosion rate just because the alloy oxygen solubility limit (all the tests are performed under oxygen saturated conditions) depends on the lead percentage in the Pb–Bi alloy.

4. Conclusion

The aim of this work was to predict the oxidation of the T91 considering that some of physico-chemical properties of the Pb–Bi alloy can locally evolve in the reactor: the temperature and the proportions of lead and bismuth in the liquid alloy. In a previous work, a predictive model of T91 oxidation in oxygen saturated LBE was performed [3,4]. This model is based on the assumption that the oxide growth rate is controlled by solid diffusion of iron in the oxide scale.

In this paper, the model is applied for other temperatures and other lead contents in the alloy in the aim to observe potential changes in the oxidation mechanism when the temperature increases and the Pb–Bi alloy composition evolves. The model applied to the different experimental conditions is compared to the T91 and Manet II oxidation results, obtained in this study and in previous studies performed at different temperatures and with different lead contents in the Pb–Bi: in LBE at 470 °C [3,4], 550 °C this study [6], 600 °C this study and 620 °C[6], in 36Pb–64Bi at 460 °C this study, in 26Pb–74Bi at 630 °C this study, in pure bismuth at 470 °C [3], in pure lead at 550 °C and 620 °C [6].

A good agreement, between experimental points oxidized in LBE and simulations, is observed whatever the temperature from 470 °C to 620 °C (deviations at high temperatures after long exposure times have to be considered). A parabolic growth kinetics is thus proposed for all the oxidation tests in LBE. The experimental oxide growth rate increases similarly as the simulated one when the temperature increases. Two conclusions emerge:

- The model forecasts the oxide growth rate in oxygen saturated LBE whatever the temperature between 470 and 630 °C.
- The temperature effect on the oxide growth rate can thus be explained with the base hypotheses of the model; it is due to the thermal activation of iron diffusion in the oxide scale.

Considering the effect of the lead content on the T91 oxidation in Pb–Bi alloy, the oxide scale characteristics are exactly the same than the ones of the oxide scale grown in LBE. Consequently, the same kind of oxidation mechanism is assumed and the model of T91 oxidation in LBE [3,4] can be applied. In this model, the composition of the liquid alloy does not contribute to the oxidation mechanism. However, because the oxygen solubility limit in the Pb–Bi alloy depends on its lead content, the liquid alloy composition fixes the oxygen activity at the oxide/Pb–Bi interface in case of oxygen saturated conditions. In this study, whatever the lead content, the experimental points are in relatively good agreement with the simulation in case of lead alloy containing bismuth or in case of pure bismuth. This is different for oxidation in pure lead for which other experiments should be performed. According to the model, this relatively good agreement means that the Pb–Bi alloy composition impacts the corrosion rate just because the oxygen solubility limit depends on the lead content.

Acknowledgement

Authors thank the European project EUROTRANS for the contribution to the financing of this work.

References

[1] L. Martinelli, F. Balbaud-Célérier, A. Terlain, S. Delpech, G. Santarini, J. Favergeon, G. Moulin, M. Tabarant, G. Picard, Corros. Sci., accepted for publication.
[2] L. Martinelli, F. Balbaud-Célérier, A. Terlain, S.Bosonnet, G. Santarini, G. Picard, Corros. Sci., accepted for publication.
[3] L. Martinelli, F. Balbaud-Célérier, G. Santarini, G. Picard, Corros. Sci., accepted for publication.
[4] L. Martinelli, F. Balbaud-Célérier, A. Terlain, S. Delpech, G. Santarini, G. Picard, in: Proceedings of EUROCORR 95, Lisboa, 2005.
[5] Handbook on lead–bismuth eutectic alloy and lead properties, materials compatibility, thermal-hydraulics and technologies, OECD, Nuclear Science, 2007, p. 129, (chapter 4).
[6] V.I. Engelko, B.P.Yatsenko, ISTC 2048. 2003.
[7] C. Fazio, G. Benamati, C. Martini, G. Palombarini, J. Nucl. Mater. 279 (2000) 308.
[8] G. Benamati, C. Fazio, H. Piankova, A. Rusanov, J. Nucl. Mater. 301 (2002) 23.
[9] C. Fazio, G. Benamati, C. Martini, G. Palombarini, Compatibility tests on steels in molten lead and lead–bismuth, J. Nucl. Mater. 296 (2001) 243.
[10] T. Furukawa, G. Müller, G. Schumacher, A. Weisenburger, A. Heinzel, K. Aoto, J. Nucl. Mater. 335 (2004) 189.
[11] G. Müller, G. Schumacher, F. Zimmermann, J. Nucl. Mater. 278 (2000) 85.
[12] G. Müller, A. Weisenburger, A. Heinzel, J. Konys, G. Schumacher, F. Zimmermann, A. Rusanov, V. Engelko, V. Martkov, J. Nucl. Mater. 335 (2004) 163.
[14] J. Töpfer, S. Aggarwal, R. Dieckmann, Solid State Ion. 81 (1995) 251.
[15] Backhaus-Ricoult, Dieckmann, Ber Bunsenges. Phys. Chem. 90, 1986, 690.
[16] Chemical reaction and equilibrium software with extensive thermochemical database, Outokumpu HSC Chemistry for Windows version 4.1, Barin 93 references.
[17] F. Gromov, B. Shmatko, J. Obninsk. 4, IPPE No ISSN 0204-3327, 1996.